MIT Open Access Articles

Biotinylated polyurethane-urea nanoparticles for targeted theranostics in human hepatocellular carcinoma

Massachusetts Institute of Technology

Research Article

Biotinylated polyurethane-urea nanoparticles for targeted theranostics in human hepatocellular carcinoma

Genoveva Morral-Ruíz[1],[§], Pedro Melgar-Lesmes[1],[†],[§], Andrea López-Vicente[1], Conxita Solans[2],[3], and María José García-Celma[1],[3] (✉)

[1] *Department of Pharmacy and Pharmaceutical Technology, Faculty of Pharmacy, University of Barcelona, Av Joan XXIII s/n, 08028 Barcelona, Spain*
[2] *Institute of Advanced Chemistry of Catalonia (IQAC), CSIC, Jordi Girona 18-26, 08034, Barcelona, Spain*
[3] *Networking Research Center on Bioengineering, Biomaterials and Nanomedicine, CIBER-BBN, Spain*
[†] *Present address: Institute for Medical Engineering and Science, Massachusetts Institute of Technology, Cambridge, MA 02139, USA*
[§] *These authors contributed equally to this work.*

ABSTRACT

Over the past years, significant efforts have been devoted to explore novel drug delivery and detection strategies for simultaneous therapy and diagnostics. The development of biotinylated polyurethane-urea nanoparticles as theranostic nanocarriers for targeted drug and plasmid delivery, for fluorescence detection of human hepatocellular carcinoma cells, is described herein. These targeted nanoparticles are specifically designed to incorporate biotin into the polymeric matrix, since many tumor types overexpress receptors for biotin as a mechanism to boost uncontrolled cell growth. The obtained nanoparticles were spherical, exhibited an average diameter ranging 110–145 nm, and showed no cytotoxicity in healthy endothelial cells. Biotinylated nanoparticles are selectively incorporated into the perinuclear and nuclear area of the human hepatocellular carcinoma cell line, HepG2, in division, but not into growing, healthy, human endothelial cells. Indeed, the simultaneous incorporation of the anticancer drugs, phenoxodiol or sunitinib, together with plasmid DNA encoding green fluorescent protein, into these nanoparticles allows a targeted pharmacological antitumor effect and furthermore, selective transfection of a reporter gene, to detect these cancer cells. The combined targeted therapy and detection strategy described here could be exploited for liver cancer therapy and diagnostics, with a moderate safety profile, and may also be a potential tool for other types of cancer.

Address correspondence to mjgarcia@ub.edu

TSINGHUA UNIVERSITY PRESS ⌂ Springer

1   Introduction

Cancer therapy and diagnostics are still scientific challenges because of the difficulty in achieving a targeted drug delivery or an accurate surgical resection of the whole tumor tissue [1]. Recent reports point to multifunctional nanoparticles as promising tools for simultaneous cancer therapy and diagnostics, that is, theranostics [2, 3]. Among the numerous developed colloidal systems, polymeric matrixes offer new possibilities to covalently bind bioactive surface molecules in order to target a specific cell type or to evade the reticuloendothelial system [4, 5]. In this regard, isophorone diisocyanate (IPDI) is a recognized monomer that can react with alcohol or amine groups, producing polyurethane-urea nanoparticles (PUR NPs) [4]. These polymeric NPs are a focus of growing interest because of their synthetic versatility, excellent mechanical properties, and high biocompatibility [6]. To date, many strategies for targeting NPs to cancer cells have been tested, including specific antibodies, proteins, or peptides [7]. Most of these strategies are aimed at binding to a cell surface target that is only upregulated in a specific type of cancer. However, cancer cells display an array of common traits to allow their permanent growth and spreading, such as angiogenesis promotion, release of matrix-degrading enzymes, and high expression of receptors and carriers for nutrients [8]. Namely, biotin receptors have been found to be highly active and overexpressed in cancer cells [9, 10]. Moreover, emerging evidence points to the participation of biotin in cell signaling, gene expression, and chromatin structure in cell proliferation [11]. Cells accumulate biotin through both the sodium-dependent multivitamin transporter and monocarboxylate transporter 1. These transporters, along with other biotin-binding proteins, drive biotin to compartments involved in metabolism, cell growth, and division. The activity of certain factors in cell signaling pathways, such as biotinyl-AMP, Sp1 and Sp3, nuclear factor (NF)-κB, and receptor tyrosine kinases is dependent on biotin supply [11]. Therefore, surface coating of PUR NPs with biotin, as we show in the present study, represents a novel strategy to obtain a targeted carrier for different cancer cells and can be useful for biomedical diagnostic or therapeutic

drug delivery to solid tumors. Furthermore, it is well known that nanoparticles under 200 nm have the additional advantage of accumulating in the tumor environment because of the enhanced permeability and retention effect (EPR) [12]. The EPR effect describes the phenomenon of accumulation of molecules with a very small size (typically liposomes, NPs, and macromolecular drugs) in the tumor microenvironment because of the unique anatomy of tumor vessels. Hence, the EPR effect is an additional aid to the transport and distribution of the NPs inside tumor tissue.

Hepatocellular carcinoma (HCC) is the third leading cause of cancer-related death worldwide and primary cause of death in patients with liver cirrhosis [13]. Curative therapies can only be offered to roughly 30% of patients, and these therapies are complicated by high recurrence rates and harsh side effects [13]. Therefore, new therapeutic strategies are urgently needed. An expert panel from the American Association for the Study of Liver Diseases has suggested that new therapies for HCC should include the combination of drugs affecting different signaling pathways or the use of multi-target approaches for molecular therapy [14]. In this context, tyrosine kinase receptors are high-affinity cell surface receptors for many polypeptide growth factors, cytokines, and hormones. These receptors have a critical role in the development and progression of many types of cancer and are being used as therapeutic candidates for multi-target drug therapy in HCC [15]. Therefore the use of drugs with multiple antitumor effects appears to be a promising approach for the treatment of HCC.

Maximal surgical resection of tumors improves patient survival [16]. However, success in surgery still relies on the surgeon's ability to delimit the presence of residual tumor tissue at the time of surgery. Neoplastic tissue limits are virtually indistinguishable from normal tissue, pointing to a clear need to improve tumor delineation during surgery. In this regard, some investigations suggest that DNA/NP hybrids are promising machinery for gene therapy and diagnostics in cancer [17, 18]. These hybrids show clear advantages in terms of the use of fluorescein or other imaging agents coated to NPs, since it is very difficult to implement feasible tumor imaging techniques, which

simultaneously offer sufficient specificity and sensitivity. Nanotechnology offers tremendous potential for medical diagnostics and novel therapeutic modalities. The combination of nanoscale materials with multi-target antitumor drugs and a reporter gene encoded by plasmid DNA could lead to the development of multifunctional medical nanoplatforms for simultaneous targeted delivery, fast diagnosis, and efficient therapy, resulting in enhanced targeting of drugs to diseased cells, as well as better monitoring of the therapeutic process. In the present study we describe the design and formation of biotinylated PUR NPs, for effective targeting of HCC cells in order to deliver multi-target drugs, and a reporter gene for simultaneous treatment and detection of these cancer cells. Current strategies in nanotechnology for linking DNA to NPs require positively charged surfaces, causing a consequential increase in toxicity to healthy cells. In contrast, our methodology does not involve a positively charged surface to bind DNA, therefore allowing better biosafety for healthy cells. Overall, this report could provide new perspectives to overcome the current limitations of therapy and diagnostics in HCC, by means of state-of-the-art nanostructure tools.

2 Experimental

2.1 Materials

Polyoxyethylene (20) sorbitan monooleate (polysorbate 80, P80) and saturated medium-chain triglycerides (MCT), as nonionic surfactant and oily component, respectively, used to prepare oil in water (O/W) nano-emulsions were supplied by Fagron (Barcelona, Spain). The isophorone diisocyanate (IPDI) monomer and the biotin used in the synthesis of PUR NPs, as well as the anticancer drugs, phenoxodiol (Phx) and sunitinib malate (STB), were purchased from Sigma-Aldrich (St. Louis, MO). The N-terminal green fluorescence protein (GFP) expression control plasmid (pcDNA3.1/NT-GFP) was supplied from Life Technologies Ltd. (Paisley, UK). One Shot® Top 10 Chemically Competent E.coli and Qiagen® Plasmid Maxi Kit, used for transformation, amplification, and purification of ultrapure, transfection-grade plasmid DNA, were purchased from Life Technologies Ltd.

(Paisley, UK) and Qiagen Inc. (Chatsworth, CA, USA), respectively. Super-optimal broth with catabolite repression (SOC) medium, Luria broth (LB broth), and LB agar ampicillin-100 plates were obtained from Sigma-Aldrich (St. Louis, MO). FuGENE® 6 Transfection Reagent to determine the transfection efficiency was supplied by Roche (Indianapolis, IN, USA).

Deionized water was obtained from a Milli-Q water purification system (Millipore, Molsheim, France).

Pig and human blood were purchased from AbD Serotec (Raleigh, NC, USA).

Primary human endothelial cells; human umbilical vein endothelial cells (HUVECs), and human hepatocellular carcinoma cells (HepG2) were supplied from Life Technologies Ltd. (Paisley, UK) and ATCC (Manassas, VA, USA), respectively. Dulbecco's Modified Eagle Medium (DMEM), Ham's F-12 Nutrient Mix (F-12), fetal calf serum (FCS), Dulbecco's phosphate buffered saline (DPBS), endothelial cell growth supplement (ECGS), and penicillin/streptomycin antibiotics were purchased from Life Technologies Ltd. (Paisley, UK).

Texas Red-conjugated goat polyclonal anti-biotin antibody and Texas Red® dye used in immunocytochemistry studies were obtained from Gene Tex Inc. (TX, USA) and Life Technologies Ltd. (Paisley, UK), respectively. Atto 565 streptavidin, employed in the detection of the biotin coated NPs, was supplied from Sigma-Aldrich (St. Louis, MO). Alexa Fluor-488 wheat germ agglutinin to stain cell membranes was purchased from Life Technologies Ltd. (Paisley, UK). The mounting medium containing 4′,6-diamidino-2-phenylindole (DAPI) was supplied from Vectashield (Vector laboratories, Burlingame, CA).

2.2 Synthesis of biotinylated polyurethane-urea nanoparticles

Biotinylated PUR NPs were obtained by the poly-addition process from O/W nano-emulsions in the water/biotin/P80/MCT/IPDI system. Briefly, 0.01 mmol of biotin was solubilized in 1.8 g of water, and then incorporated, drop wise, at 25 °C to MCT/P80/IPDI mixtures (0.02 g/0.18 g/0.04 mmol, using an oil/surfactant weight ratio of 10/90), under continuous mechanical stirring at 2,500 rpm to obtain O/W nano-emulsions. Samples were then immediately heated

at 70 ± 2 °C in a thermostatic bath for 4 h to achieve biotinylated PUR NPs. Afterwards, NPs were freeze-dried (Freeze-Dryer Lyoquest, Telstar) and reconstituted with 1.8 mL of DPBS just before use for the individual studies [19].

Phx-loaded and STB-loaded biotinylated PUR NPs were prepared by solubilizing 1,000 μg of anticancer drug into 0.2 g of MCT/P80/IPDI mixture. Then, 1.8 g of water solution containing 0.01 mmol of biotin was incorporated stepwise to these mixtures, stirring continuously until O/W nano-emulsions with a final concentration of 90 wt% aqueous component-were obtained. Nanoparticles were obtained by heating these samples at 70 ± 2 °C. The polyaddition process was completed after 4 h, and then samples were freeze-dried and reconstituted as described above.

To obtain biotinylated PUR/pc DNA complex, 2,000 μg plasmid pcDNA3.1/NT-GFP was previously solubilized in 100 μL of water and then incorporated into MCT/P80/IPDI or MCT/P80/IPDI/drug mixtures. Then, 1.7 g of the aqueous component (biotin/water solution at 1/90 weight ratio) was stepwise added to form the O/W nano-emulsions. Polyaddition was induced by heating samples at 70 ± 2 °C for 4 h, and biotinylated PUR/pc DNA complexes were obtained. Samples were freeze-dried and reconstituted with DPBS, for all studies. Transformation, amplification, and purification processes to obtain ultrapure, transfection-grade plasmid DNA were carried out following the protocols described in the Qiagen® Plasmid Maxi Kit. Plasmid concentration was quantified at 260 nm by spectrophotometry, using the Take3 micro-volume plate attached to an Epoch spectrophotometer (Biotek Instruments, Winooski, VT, USA).

2.3 Physicochemical characterization of nanoparticles

Nanoparticle size properties were determined by dynamic light scattering (DLS), using a Zetasizer nano ZS (Malvern Instruments Ltd., UK). Measurements were carried out at 25 °C and at fixed angle of 173°, by analyzing the intensity of the scattered light supplied by a helium-neon laser (4 mW, $\lambda = 633$ nm). The DLS data were calculated from the autocorrelation function of scattered light by means of two mathematical approaches; the cumulants method and the non-

negatively constrained least squares (NNLS/Contin) algorithm, using the Dispersion Technology Software nano v. 5.10 (Malvern Instruments Ltd.). Through the cumulants analysis, two important parameters are obtained; the mean hydrodynamic diameter of the NPs (Z-Average) and the width of the particle size distribution (Polydispersity index-PDI). To prepare samples for the measurements, 20 μL of NP suspension was dispersed in 1,480 μL of DPBS, in an ordinary cuvette. Reported values of Z-Average and PDI corresponded to the average of approximately 40 measurement runs.

Stability studies of biotinylated PUR NPs were carried out by DLS at 25 °C, measuring the mean particle diameter of NP dispersed in culture medium as a function of time, for 2 months. Samples were kept at 4 °C throughout the studied period (62 days) and were left to acclimatize at 25 °C before the measurements.

The size and morphology of different NPs were characterised by TEM, using a JEOL JEM 1010 microscope (JEOL, Akishima, Japan) equipped with an AMT XR40 digital imaging camera, at a magnification of 75,000× and a maximum accelerating voltage of 100 kV. In prior observation, one droplet of NP suspension was placed on a carbon-coated copper grid, and negative staining with an aqueous solution of uranyl acetate at 1% (*w/v*) was conducted. Particle diameter of approximately 300 randomly selected NPs from different TEM images was determined using the morphometry software ImageJ v. 1.44 (U.S. National Institutes of Health, Bethesda, Maryland, USA).

The incorporation and integrity of biotin in biotinylated polyurethane NPs was detected by fluorescence, using a fluorescence confocal microscope (Leica TCS SP2, Leica Microsystems, Wetzlar, Germany). Briefly, non-biotinylated (negative control) and biotinylated PUR NPs were incubated overnight at 4 °C with Atto 565 streptavidin complex (1/200). After incubation, 20 μL of sample was placed on a microscope slide and mounted with a coverslip for observation.

2.4 Cell culture

HUVECs were cultured in pre-gelatinized plates with DMEM/F-12 medium supplemented with 10% FCS, 50 U·mL^{-1} penicillin/streptomycin and 50 μg·mL^{-1}

ECGS. Cells were grown at 37 °C and 5% CO_2, in a water jacketed incubator (Heracell 150i, Thermo Scientific, Pittsburgh, USA). HUVECs were passaged when they reached 80% confluence and passages 2–5 were used for all experiments.

HepG2 cells were cultured with DMEM supplemented with 10% FCS and 50 U·mL⁻¹ penicillin/streptomycin. Cells were grown at 37 °C and 5% CO_2, in a water jacketed incubator (Heracell 150i, Thermo Scientific, Pittsburgh, USA).

2.5   Biological characterisation of nanoparticles

The hemocompatibility of NPs was evaluated through the *in vitro* red blood cell (RBC) hemolysis test [20]. Thereby, an erythrocyte fraction was collected from fresh pig and human blood after being centrifuged at 5,100 x g, for 10 min, at 4 °C (Heraeus Megafuge 16R centrifuge, Thermo Scientific, Pittsburgh, USA), and then washed three times with DPBS to obtain a final stock dispersion of 3 mL of remaining packed erythrocytes dispersed into 11 mL of DPBS. Samples for analysis were prepared by incorporating 100 μL of stock erythrocyte dispersion into 1 mL of the NP suspension. Previously, freeze-dried NPs were reconstituted in DPBS and then weakly diluted in deionized water, to guarantee the isotonicity of the NP suspension (osmolality values ranging 280–300 mOsm·mL⁻¹). The samples were then incubated for 10 min at 37 °C in an Incubator Shaker and after that centrifuged for 5 min at 18,000 x g (IEC MicroCL 21R centrifuge, Thermo Scientific, Pittsburgh, USA). The percentage of hemolysis was obtained by comparing the absorbance (λ = 540 nm) of the supernatant with control samples totally hemolysed with 1 mL of deionized water, as previously reported. The blank consisted of a blood sample not treated with NPs and incubated with 1 mL of DPBS, to obtain only the percentage of particle-induced hemolysis. Experiments were repeated five times for each sample.

The cytotoxicity of NPs on cell viability of HUVECs and HepG2 was assessed using the CellTiter96 Aqueous One Solution Cell Proliferation Assay (MTS assay, Promega, Madison, WI, USA). Briefly, cells were seeded in 96-well plates (pre-gelatinized only for HUVECs) at a cell density of 5×10^3 cells per well and incubated for 24 h in the corresponding complete media, as described above. Then, cells were serum-starved for 6 h and afterwards were co-incubated with 8.5 mg·mL⁻¹ or 1 mg·mL⁻¹ of NPs for 24 h, at 37 °C. Just before determination of cell viability, cells were washed with DPBS and transferred into starvation medium. Cytotoxicity was determined by adding 20 μL of MTS solution to each well. After 2 h, the absorbance was measured at 490 nm using an Epoch microplate spectrophotometer (Biotek Instruments, Winooski, VT, USA). Cell viability was expressed as the absorbance of cells treated with NPs relative to cells treated with DPBS (control cells). Each condition was performed in sextuplicate and reported as mean ± SEM.

2.6   Immunocytofluorescence studies

HepG2 and HUVECs were seeded in 2-well Labtek II chamber slides (Thermo Scientific, Pittsburgh, USA) and grown to 80% confluence. Thereafter, cells were incubated with fresh complete medium in the presence of 1 mg·mL⁻¹ of biotinylated PUR NPs or non-biotinylated PUR with Texas Red dye-incorporated NPs for 8 h. After that, cells were washed three times with tris-buffered saline (TBS) to keep only endocyted NPs, and then cell cultures were fixed with a 1% zinc solution for 30 min, at room temperature. Cell slides were then incubated with Texas Red-conjugated goat polyclonal anti-biotin antibody (1/200) and Alexa Fluor-488 wheat germ agglutinin (1/2,500). In addition, DAPI mounting medium was used to counterstain cell nuclei. Positive signal was detected with a fluorescence confocal microscope (Leica TCS SP5, Leica Microsystems, Wetzlar, Germany).

2.7   Transfection studies

The transfection efficiency of biotinylated PUR/pc DNA complexes and the commercial   kit FuGENE 6 was studied in both HepG2 cells and HUVECs.

According to the instructions of the FuGENE® 6 kit, cells were seeded at a concentration of 5×10^4 cells in 2-well Labtek II chamber slides and grown with the corresponding complete media to 50-80% confluence. After that, cells were serum-starved for 6 h and co-incubated with 10 μg·mL⁻¹ of plasmid DNA, 1 mg·mL⁻¹ of biotinylated PUR/pc DNA complex (this concentration of NPs correspond to 10 μg·mL⁻¹ of

plasmid DNA) or FuGENE® 6 Reagent at a plasmid concentration of 10 μg·mL^{-1} μg/mL and maintaining a FuGENE® 6/DNA ratio of 3/1, for 8 more hours. Afterwards, cells were washed with DPBS and incubated with the corresponding complete medium for 48 h to achieve the maximum expression of the GFP. Prior to the observation by fluorescence confocal microscope, cells were washed with tris-buffered saline (TBS), fixed with a 1% zinc solution for 30 min at room temperature and placed on a microscope slide and mounted with a coverslip using a DAPI mounting medium to counterstain cell nuclei.

2.8 Cell proliferation assays

The effect of designed NPs on cell proliferation was tested in tumor cells (HepG2) as in healthy vascular cells (HUVEC).

Thereby, cells were seeded in 96-well plates (previously pre-gelatinized for HUVECs) at a cell density of 5×10^3 cells per well and incubated for 24 h in the corresponding complete media. After that, cells were co-incubated in fresh medium with DPBS, the anticancer drugs, or NP formulations at a concentration of 1 mg·mL^{-1}, for a period of 8 h. The anticancer drug concentrations selected for this study were 20.81 μM for Phx and 9.38 μM for STB, and corresponded to the drug concentrations loaded into 1 mg·mL^{-1} of NPs. On the other hand, the dose-response profiles of the designed theranostics on tumor cell samples at drug concentrations of 41.62 μM, 10.40 μM, and 5.20 μM for Phx, and 18.77 μM, 4.69 μM, and 2.34 μM for STB were also assessed. Afterwards, cells were washed three times with DPBS to maintain only the particles that had been taken up, and then transferreed to serum-free medium for a total period of 24 h, to allow the drug to arrest the proliferation. Twenty microliters of MTS solution was then incorporated into each well for determining the absorbance at 490 nm, after 2 h, using an Epoch microplate spectrophotometer. Cell viability was calculated as the absorbance of nanoparticle-treated cells relative to control cells (treated with DPBS). Each condition was performed in sextuplicate and reported as mean ± SEM.

2.9 Statistical analysis

All data were expressed as mean ± standard error (SEM). Statistical analysis of the results was performed by one-way analysis of variance (ANOVA) and the Newman-Keuls test. Differences were considered to be statistically significant at a p-value $\leqslant 0.05$.

3 Results and Discussion

3.1 Design and characterization of biotinylated polyurethane-urea nanoparticless loaded with a reporter gene-containing plasmid and either sunitinib or phenoxodiol

The synthetic procedure to obtain theranostic biotinylated polymeric NPs loaded with a reporter gene plasmid and one antitumor drug is presented in Fig. 1(a). NPs with a biotin-coated surface were achieved via a polyaddition process from O/W nano-emulsions prepared by the phase inversion composition (PIC) emulsification method in the water/biotin/polysorbate 80/saturated medium chain triglyceride/diisocyanate system. The use of biotin to functionalize the polymeric matrix is an elegant strategy to achieve a multi-tumor nanocarrier, which is able to target cancer cells which have a huge requirement for biotin in order to expand and invade the environment. Thereby, taking advantage of the high binding and uptake of biotin, we designed selective nanoplatforms to deliver a reporter gene and an antitumor drug to identify and kill cancer cells, respectively (Fig. 1(a)).

Biotin receptors are overexpressed in cancer cells and can allow the binding of these biotinylated nano-particles, facilitating their internalization, thus delivering the plasmid for green fluorescent protein (GFP) expression, and a multi-target drug (STB or Phx) to attack the hepatoma cell, as shown in Fig. 1(b). Both STB and Phx have demonstrated to be powerful multi-target anticancer drugs, through different mechanisms of action, but have also shown harmful side effects, in clinical studies [21, 22]. This means that they are potential candidates to be employed in targeted nanocarriers for the improvement of their selectivity, as well as their efficiency, in treating human cancers. Moreover, the design of tumor-targeted NPs loaded with a reporter gene can provide precise identification of the extent of the tumor tissue to be surgically excised.
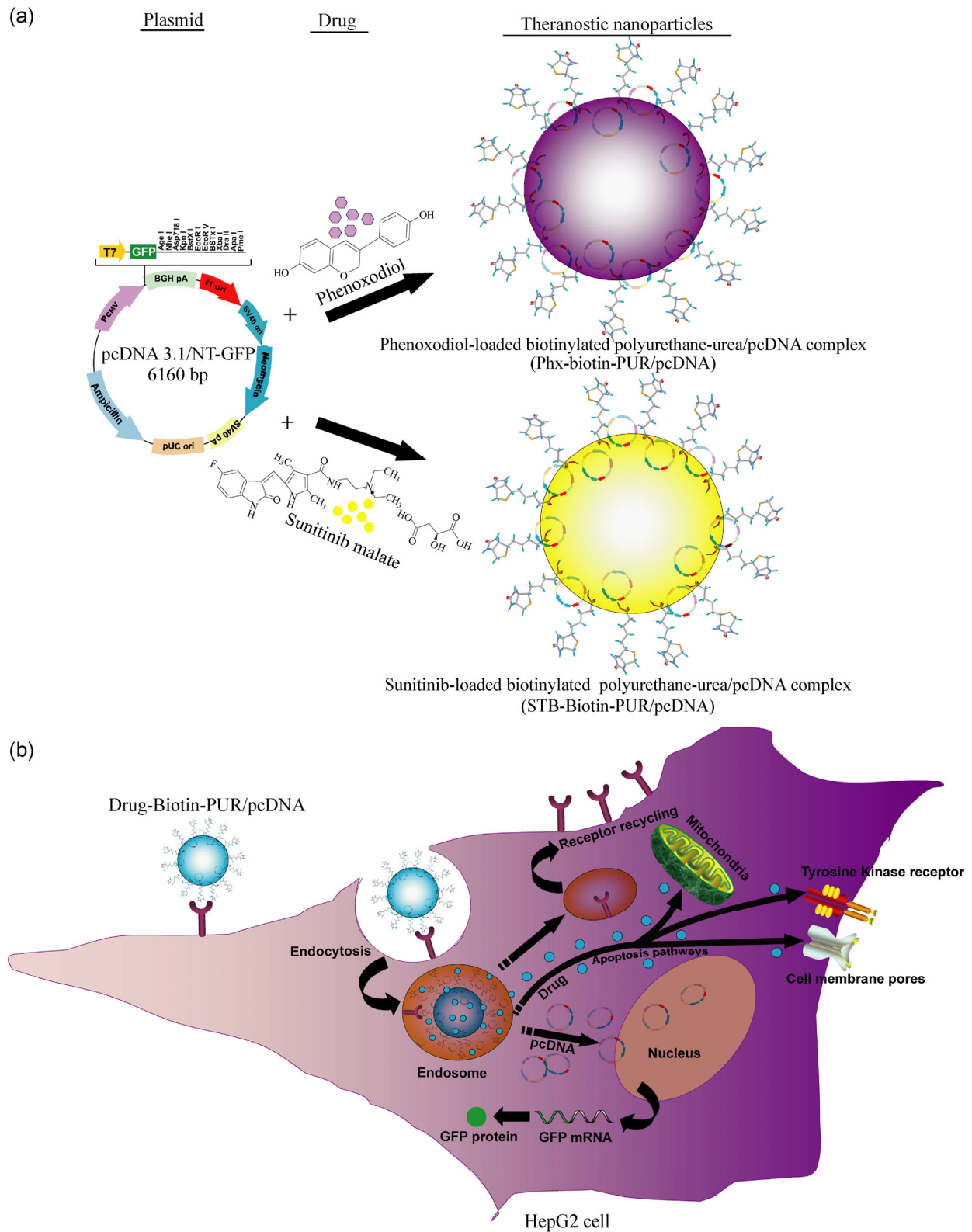
(a)

Plasmid

Drug

Theranostic nanoparticles

pcDNA 3.1/NT-GFP
6160 bp

Phenoxodiol

Phenoxodiol-loaded biotinylated polyurethane-urea/pcDNA complex
(Phx-biotin-PUR/pcDNA)

Sunitinib malate

Sunitinib-loaded biotinylated polyurethane-urea/pcDNA complex
(STB-Biotin-PUR/pcDNA)

(b)

Drug-Biotin-PUR/pcDNA

Receptor recycling

Mitochondria

Tyrosine Kinase receptor

Endocytosis

Drug

Apoptosis pathways

Cell membrane pores

Endosome

pcDNA

Nucleus

GFP protein

GFP mRNA

HepG2 cell

Figure 1 Design, uptake, and multi-targeting of biotinylated theranostic nanoplatforms. (a) Design of theranostic nanoparticles with anticancer drugs, phenoxodiol or sunitinib malate, and DNA plasmid encoding green fluorescence protein (GFP). (b) Theoretical mechanism of specific targeting and uptake of theranostic biotinylated polyurethane-urea nanoparticles loading anticancer drugs and plasmid DNA, on human hepatoma cells (HepG2).

Biotinylated PUR NPs designed in the present study were thoroughly characterized. It is well known that nanoparticle size plays a key role in cellular uptake, interaction with plasma proteins, drug release, toxicity, and molecular response [23]. Therefore, size properties of biotinylated NPs, such as mean hydrodynamic diameter and polydispersity index, were determined by DLS at 25 °C (Table 1). Likewise, morphological properties of NPs were also evaluated by TEM, as shown in Fig. 2.

As shown in Table 1, NPs exhibited mean hydrodynamic diameters ranging between 110–145 nm, with narrow particle size distributions (PDI ⩽ 0.15). Morphological studies by TEM (Fig. 2) evidenced the formation of homogeneous populations of isometric, spherical shaped NPs with continuous, clearly defined limits and estimated particle diameters in the range of 76–112 nm. As expected [4], these particle sizes

were lower than those measured by DLS, since this technology actually determines the hydrodynamic diameter, whereas data from TEM image analysis provide hard-sphere diameters. Tumor targeting carriers must be small enough to penetrate through transvascular pores and fenestrations in order to reach the tumor environment. In this regard, it has been reported that the minimum sizes measured for pore cutoff, for a limited number of tumor models, are around 200–400 nm [24, 25]. Therefore, biotinylated nanoparticles with diameters below 150 nm would meet the required size properties to be easily accumulated in tumor vasculature, taking advantage of the enhanced permeability and retention (EPR) effect.

To evaluate the impact of the culture medium components on the size properties, particle diameter of biotinylated PUR NPs dispersed in HepG2 culture medium was measured by DLS for 62 days (Fig. S1(a)
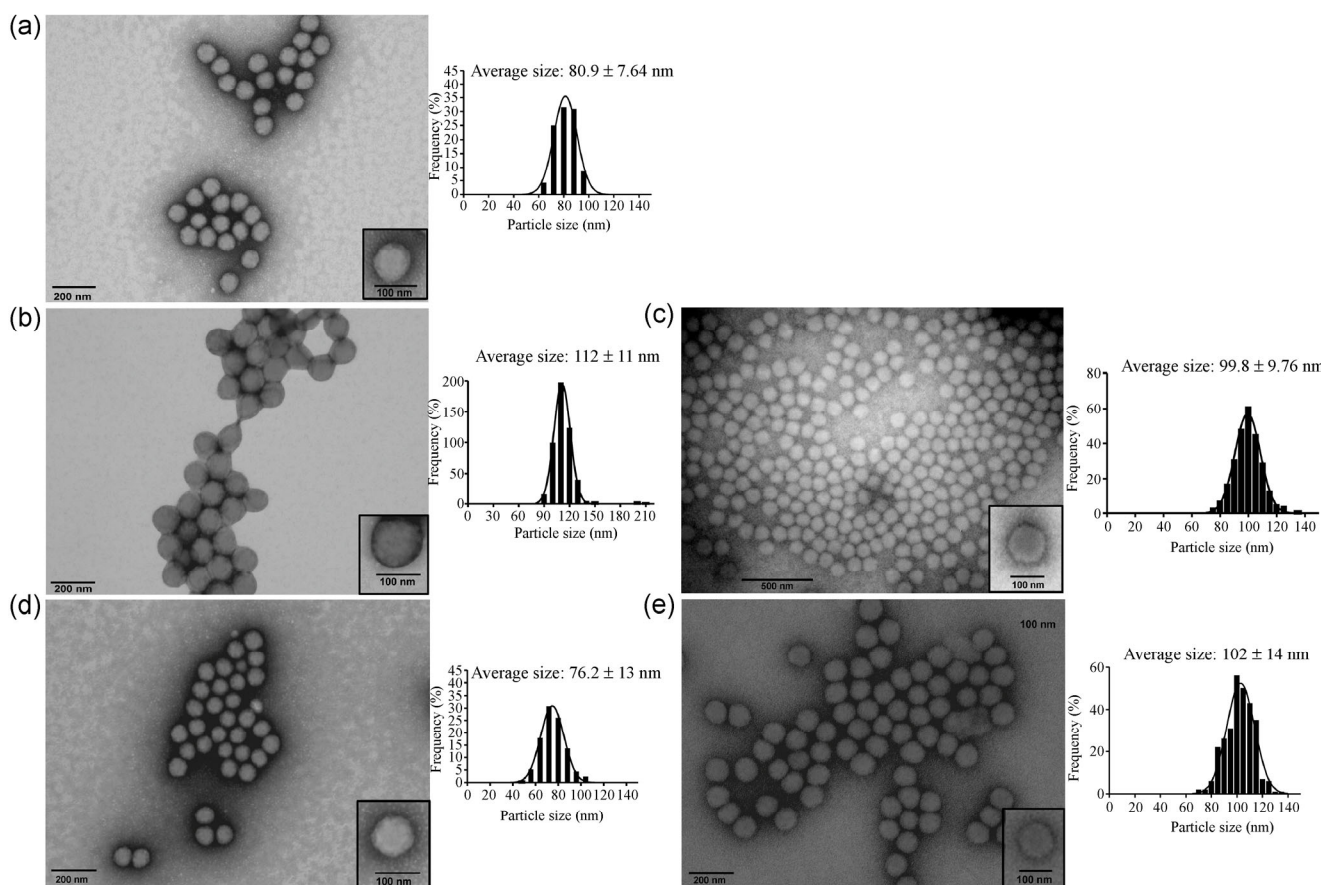

Figure 2 Characterization by transmission electron microscopy (TEM) of biotinylated polyurethane-urea (PUR) nanoparticles (NPs). Micrographs and particle size distribution curves of biotinylated PUR/pc DNA complex (a), phenoxodiol-loaded biotinylated PUR (b), phenoxodiol-loaded biotinylated PUR/pcDNA complex (c), sunitinib-loaded biotinylated PUR NPs (d) and sunitinib-loaded biotinylated PUR/pcDNA complex (e).

Table 1 Size properties (hydrodynamic diameter (Z-Average) and polydispersity index (PDI)) of the designed biotinylated polyurethane-urea nanoparticles

Samples[a]	Z-Average (nm)[b]	PDI[b]
Biotinylated polyurethane-urea/pc DNA complex (Biotin-PUR/pcDNA)	120.2 ± 1.8	0.14
Phenoxodiol-loaded biotinylated polyurethane-urea (Phx-Biotin-PUR)	145.1 ± 1.4	0.11
Phenoxodiol-loaded biotinylated polyurethane-urea/pcDNA complex (Phx-Biotin-PUR/pc DNA)	142.6 ± 1.5	0.15
Sunitinib -loaded biotinylated polyurethane-urea (STB-Biotin PUR)	114.5 ± 1.2	0.11
Sunitinib-loaded biotinylated polyurethane-urea/pcDNA complex (STB-Biotin-PUR/pcDNA)	110.9 ± 1.0	0.10

[a] Nanoparticles were synthesized by polyaddition from O/W nano-emulsions with 90 wt% and an oil/surfactant weight ratio of 10/90 in the water/biotin/ polysorbate 80/saturated medium chain triglyceride/diisocyanate system; [b] Z-Average and PDI of nano-particles were determined by dynamic light scattering at 25 ℃, though the cumulants analysis.

in the Electronic Supplementary Material (ESM)). NPs exhibited moderate kinetic stability during the entire study period. Nevertheless, a slight increase of the particle diameter, around 15 nm, was produced during the first 20 days. This stability profile is in accordance with the stability results obtained for analogous PUR nanoparticulate systems in aqueous dispersion, thus attributing this increase in particle size to swelling phenomena during storage at 4 ℃ [19, 26]. Furthermore, the stability of biotinylated PUR NPs against aggregation and swelling phenomena was considerably improved after the freeze-drying process, thus allowing the storage of the samples even for a long period (2 years) without any modification of size properties (Fig. S1(b) in the ESM).

The specific uptake of the designed nanovectors by cancer cells could be enhanced by conjugating the nanocarrier with different ligands, such as peptides, proteins, and antibodies. In this context, biotin would offer a wide array of possibilities, allowing not only a selective targeting to different kinds of cancerous cells but also an increase of cellular internalization of NPs and a depletion of the reticuloendothelial system uptake [27]. The successful incorporation and integrity of the biotin in PUR NPs was corroborated by fluorescence confocal microscopy after incubating NPs with Atto 565 streptavidin complex (Fig. S2 in the ESM). A fluorophore conjugated to streptavidin was selected because of the high specificity of biotin to bind to this protein. Thereby, the detection of positive signal (red fluorescence) attributed to the fluorophore Atto 565 was indicative of successful incorporation of biotin into NPs. Moreover, this revealed that specific binding sites of biotin for streptavidin were preserved and intact after the polymerization process (Fig. S2(b)). In addition, no fluorescence was observed after incubating bare PUR NPs (without biotin) with Atto 565 streptavidin complex (Fig. S2(a)).

The biosafety of any nanomedicine to come into contact with different biological interfaces before reaching its therapeutic goal places great importance on the designed nanocarriers being safe and innocuous, causing no potential damage to these biological structures. To study the biocompatibility of NPs, hemolysis and cytotoxicity studies were performed in erythrocytes of porcine and human origin, and in two human cell lines (HUVEC and HepG2) (Fig. S3 in the ESM). Biotinylated PUR NPs did not show any hemolytic effects, either in pig or human erythrocytes, demonstrating moderate hemocompatibility. On the other hand, NPs also showed a high biocompatibility, since no cytotoxicity in HUVECs was observed in the MTS assay after being exposed for 24 h at 1 mg·mL^{-1} (Fig. S3). Hence, NPs described in the present study exhibited a moderate biosafety profile, which makes them suitable to be intravenously administered.

3.2 Specific uptake and perinuclear localization of biotinylated PUR NPs in human hepatocellular carcinoma cells

To find out whether functionalization with biotin could specifically boost the incorporation of PUR NPs in hepatoma cells, we incubated bare NPs loaded with Texas Red fluorescent dye and biotinylated NPs with the hepatoma cell line HepG2 and the vascular healthy endothelial cell line HUVEC (Fig. 3).

As shown in Figs. 3(a) and 3(c), NPs lacking biotin were barely incorporated into tumor and healthy vascular cells. In contrast, biotinylated NPs were successfully endocyted in HepG2 cells and accumulated
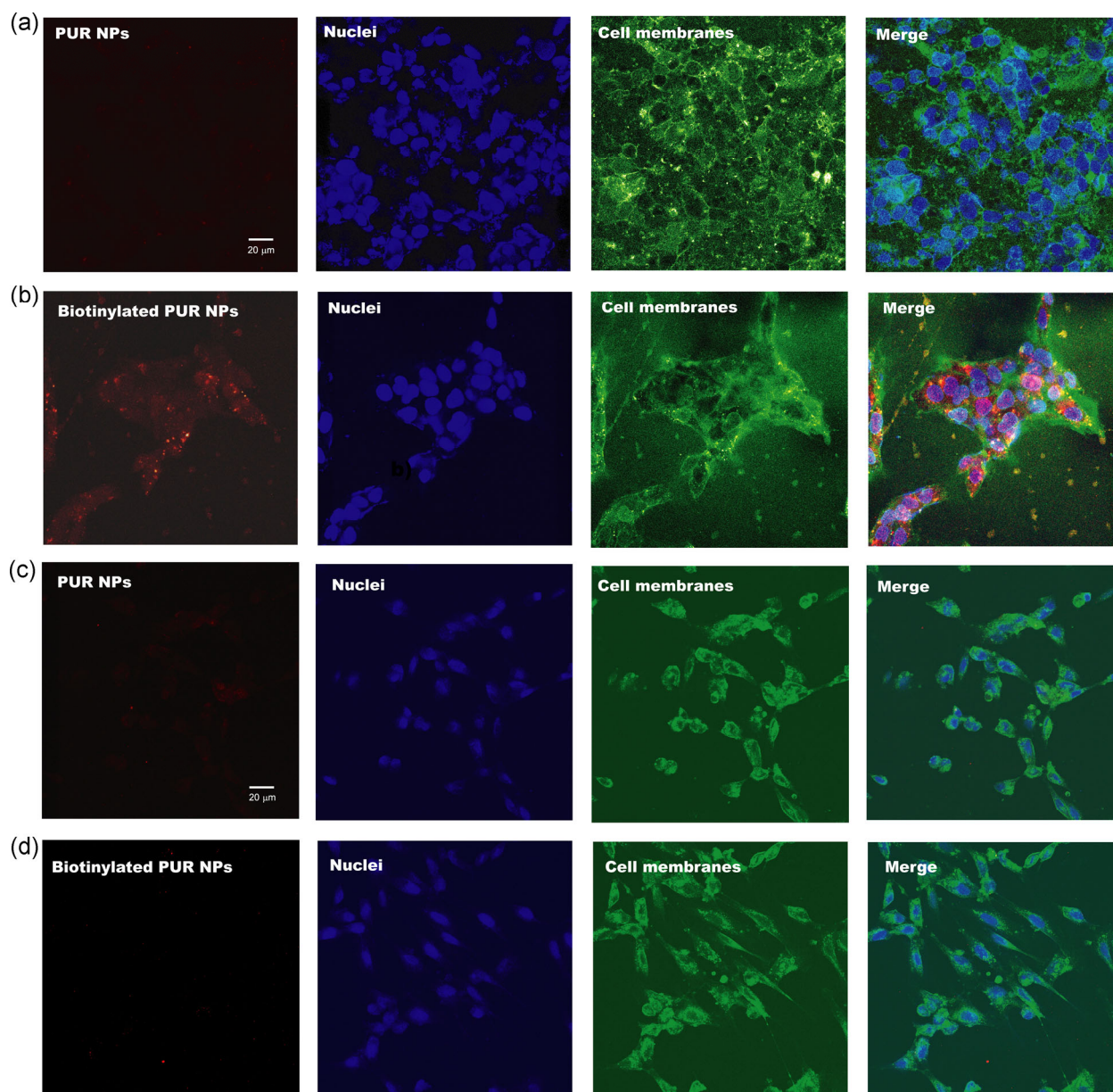
Figure 3 Fluorescent detection of specific uptake and internalization of biotinylated polyurethane-urea (PUR) nanoparticles (NPs) in human hepatoma cells (HepG2). Images for (a) and (b) correspond to immunocytofluorescence studies carried out in HepG2 cells, and (c) and (d) to experiments developed in vascular healthy cells (HUVEC). Cells were treated with bare PUR NPs, encapsulating Texas Red dye ((a) and (c) images) or with biotinylated PUR NPs ((b) and (d) images), at a concentration of 1 mg·mL^{-1}. Immunofluorescent detection of NPs is shown in red, cell membranes in green, and cell nuclei in blue.

close to or within the cell nuclei (Fig. 3(b)). Moreover, this uptake and internalization was specific for these malignant cells, since extremely low red fluorescent signal attributed to the endocytosis of biotinylated PUR NPs was observed in HUVECs (Fig. 3(d)). Therefore, biotinylation of NPs appears to be a feasible strategy that offers an array of possibilities, not only for targeting cancer cells in order to deliver drugs, but

also for gene therapy. Moreover, biotinylated NPs can be detected by streptavidin-coated imaging agents, specific anti-biotin antibodies, or a combination of both systems. This fact potentiates the number of combinations in which a drug or a gene of interest can be loaded into this type of functionalized NP to achieve a targeted therapy and simultaneous diagnosis (theranostics). Indeed it is especially important for the

complete resection of the tumor tissue. Current cancer therapy usually involves chemotherapy together with surgery to remove the tumors, if possible, because maximal surgical resection of the tumor may improve survival [28]. Nevertheless, success of the surgery relies on the surgeon's ability to visually distinguish the presence of residual tumor tissue at the time of surgery [29]. Unfortunately, it is very difficult to implement feasible tumor imaging techniques that simultaneously offer sufficient specificity and sensitivity. For that reason the possibility to differentiate between the whole tumor mass and the healthy tissue using biotinylated NPs, which can be easily coupled to imaging agents, can improve the resection process by tumor delineation during surgery, with minimal or no side-effects. Investigators have proposed the use of multiple imaging agents to aid the recognition of neoplastic tissue during resection [30, 31]. We have shown that imaging agents, coupled to biotinylated NPs, can be accumulated in hepatoma cells to help identify the tumor tissue.

3.3 Efficient transfection of plasmid DNA-biotinylated NPs and expression of a reporter gene in HepG2 cells

To assess the potential efficacy of gene transfection of biotinylated NPs in human hepatocellular carcinoma, we incorporated plasmid DNA encoding GFP into these NPs, and these were then incubated with HepG2 cells. In order to establish a range for efficiency, we incorporated the same concentration of plasmid (10 μg·mL^{-1}) in a commercial kit for transfection (FuGENE® 6) and these constructs were incubated with HepG2 cells in the same conditions. Results are shown in Fig. 4.

No GFP expression was observed in cancer cells incubated with plasmid DNA alone (Control, Fig. 4). In contrast, most of the cells expressed GFP after incubation with DNA incorporated into the commercial transfection reagent (FuGENE® 6, Fig. 4). Surprisingly, the incorporation of plasmid DNA into biotinylated NPs resulted in a much higher synthesis of GFP in HepG2 cells than the commercial kit (biotinylated PUR, Fig. 4). This is most likely a consequence of the selective accumulation of these NPs into the nucleus and its vicinity, hence boosting the rate of transcription

of messenger RNA producing GFP, and therefore exponentially increasing the synthesis of GFP. Transfection kits like FuGENE® 6 use liposomes to transfer the plasmid DNA, taking advantage of the properties of lipid bilayers to fuse with the cell membrane to deliver the DNA. However, this strategy is not mediated by a targeted and selective delivery into the cancer cell, and it is completely dependent on a fixed and passive rate of uptake. According to our data, the coating of plasmid DNA to biotinylated NPs can have great value either for gene therapy in HCC or for designing better commercial kits of DNA transfection for cancer cells. Moreover, taking advantage of the wide array of ligands, which can be linked to these polymeric nanoparticles, different strategies could be used to enhance transfection efficiency when needed. In this regard, phosphate calcium and virus capsid components (adenovirus or retrovirus) have demonstrated to be highly effective systems to increase gene delivery [32, 33] and could easily be incorporated into our formulations, to boost transfection efficiency.

3.4 The transfection of plasmid DNA-biotinylated NPs is not boosted in healthy human endothelial cells

To evaluate whether the uptake of biotinylated NPs and therefore, the selective transcription of plasmid DNA, was selective in cancer cells, we incubated plasmid DNA-biotinylated NPs and DNA-FuGENE® 6 with vascular healthy cells (isolated HUVECs) (Fig. 5). Endothelial cells are the primary cell barrier in blood vessels and consequently, are the first biological point of contact with an intravenously administered formulation. In this regard, it is very important to avoid the common undesired effect of peripheral vascular toxicity due to the low cell selectivity of traditional drug therapies in cancer [34].

We did not observe GFP synthesis in HUVECs incubated with plasmid DNA alone (Control, Fig. 5). On the contrary, roughly 60% of HUVECs expressed GFP after incubation with DNA incorporated with the transfection kit (FuGENE®6, Fig. 5). On the other hand, plasmid DNA-biotinylated NPs showed much lower synthesis of GFP in HUVECs than the commercial kit (biotinylated PUR, Fig. 5). GFP presence was detected at very low levels and in less than
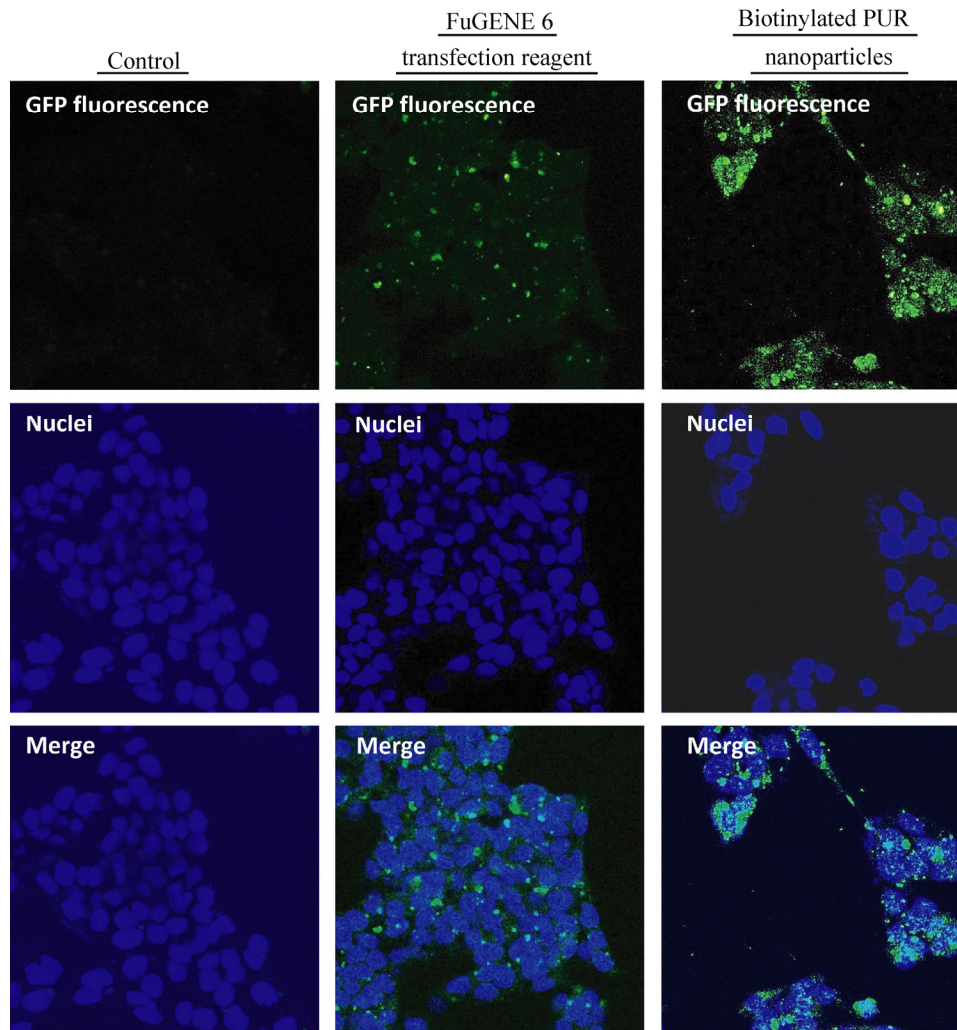
Figure 4   Transfection efficiency and GFP expression of biotinylated polyurethane-urea (PUR)/plasmid DNA complex and commercial transfection reagent in human hepatocellular carcinoma cell (HepG2), observed by confocal microscopy. Cells were incubated for 8 h with 10 µg·mL^{-1} of plasmid pcDNA3.1/NT-GFP, with FuGENE® 6 transfection reagent incorporating 10 µg·mL^{-1} plasmid DNA, or with 1 mg·mL^{-1} of biotinylated PUR/pc DNA complex loaded with 10 µg·mL^{-1} of DNA. Expression of GFP was evaluated after 56 h of treatment. Cell nuclei are stained in blue, with DAPI, and the expression of GFP is shown as green fluorescence.

5% of HUVECs. This means that both the therapeutic and diagnostic potential properties of biotinylated NPs are selective for human hepatoma cells and are not expected to have toxic effects on vasculature, or false positives, in the labelling of tumor tissue.

3.5   Targeted anti-proliferative effects of biotinylated PUR NPs loaded with sunitinib or phenoxodiol, in human hepatoma cells

To assess the potential of biotinylated PUR NPs to lead a targeted drug delivery effect, aside of gene therapy, we incorporated the anticancer drugs: sunitinib and

phenoxodiol. STB is a multi-target receptor tyrosine kinase inhibitor that has been tested as an anti-proliferative drug in a wide array of cancers [35–37], including hepatocellular carcinoma [21].

Similarly, Phx is an anticancer drug that promotes cancer cell death through many different mechanisms and pathways [38–40]. The multi-target properties of anticancer drugs are essential to avoid adaptation of cancer cells to the therapy and tumor recurrence. Moreover, a major bottleneck in cancer therapy lies in achieving specific drug accumulation at tumor tissue, because most chemotherapeutic agents are unable to
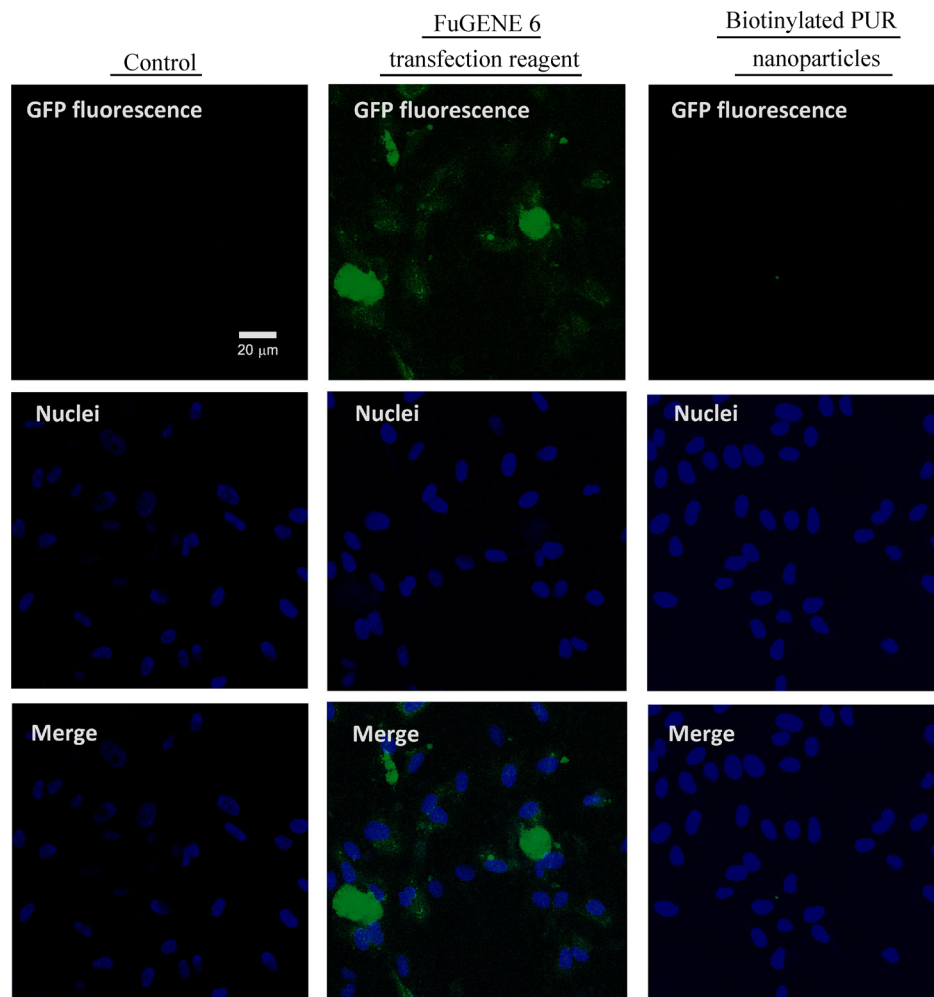
Figure 5   Transfection efficiency and GFP expression of biotinylated polyurethane-urea (PUR)/plasmid DNA complex and commercial transfection reagent in vascular healthy cells (HUVEC), evaluated by fluorescence confocal microscopy. Cells were treated for 8 h with 10 $\mu g \cdot mL^{-1}$ of plasmid pcDNA3.1/NT-GFP, with FuGENE® 6 transfection reagent containing 10 $\mu g \cdot mL^{-1}$ plasmid DNA, or with 1 $mg \cdot mL^{-1}$ of biotinylated PUR/pc DNA complex loaded with 10 $\mu g \cdot mL^{-1}$ of DNA. Expression of GFP was observed after 56 h of treatment. Cell nuclei are stained in blue, with DAPI, and the expression of GFP is shown in green.

differentiate between diseased and healthy cells, leading to poor biodistribution and undesired side effects. This obstacle could potentially be overcome by targeted delivery systems. For this reason, we designed different therapeutic strategies, based on biotinylated NPs (Biotinylated PUR NPs, Biotinylated PUR/pcDNA complex, Phx-loaded biotinylated PUR NPs, Phx-loaded biotinylated PUR/pcDNA complex, STB-loaded biotinylated PUR NPs and STB-loaded biotinylated PUR/pcDNA complex), and tested them in both HepG2 cells and HUVECs, as shown in Fig. 6.

According to the results (Fig. 6), both biotinylated PUR NPs loaded with Phx and the theranostic coupling

of Phx + plasmid promoted an approximately 20% reduction in HepG2 cell proliferation after 8 h of uptake and a total of 24 h of treatment, as compared with Phx in suspension (Fig. 6(a)). The exposure time is around six times lower than those previously reported because we aimed to potentiate the targeted effects and to prevent any possible side effects [41]. In fact, we also demonstrated that none of the formulations incorporating Phx were able to induce any toxic effects in cell proliferation of HUVECs after 8 h of exposure (Fig. 6(b)). Similarly, only biotinylated PUR NPs loaded with sunitinib or coupled sunitinib + plasmid significantly reduced the proliferation of
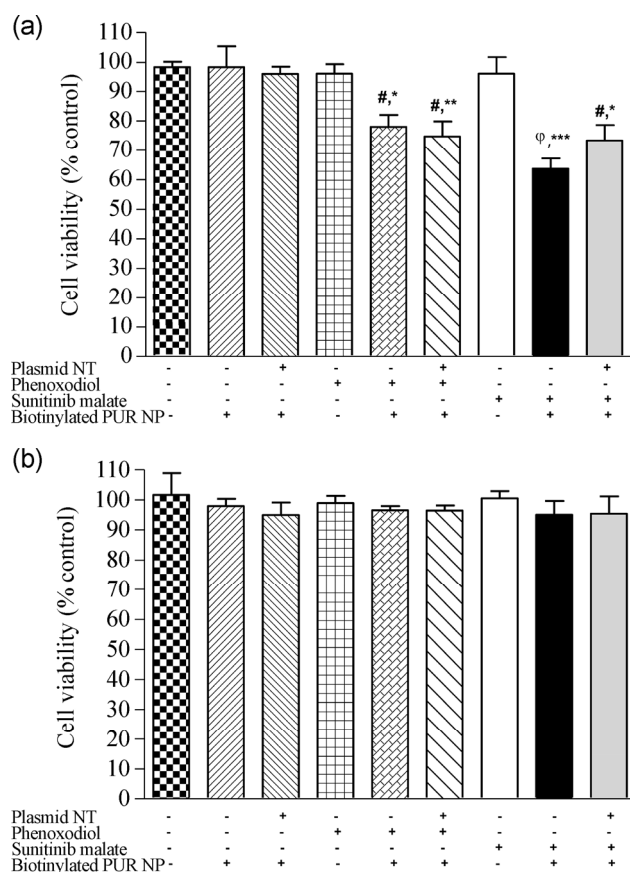
Figure 6 Evaluation of the specific antiproliferative effects of anticancer drug (phenoxodiol or sunitinib malate)-loaded biotinylated polyurethane-urea (PUR) nanoparticles (NPs) in human hepatoma cells (HepG2) and healthy endothelial cells (HUVEC). Antiproliferative effects assessed in (a) HepG2 cells and (b) HUVECs. Cell proliferation was determined by the CellTiter96 Aqueous One Solution Cell Proliferation Assay (MTS assay) after treating cells directly with the antitumor drugs, with 1 mg·mL^{-1} of drug-loaded biotinylated PUR NPs or with 1 mg·mL^{-1} of theranostic NPs (drug-loaded biotinylated PUR/ pcDNA complex). All tested formulations were incubated for 8 h, then washed and incubated again for 24 h, to evaluate the specific proliferative arrest of only internalized NPs. Each column represents the mean ± SEM. # $p < 0.01$, φ $p < 0.0001$ as compared with control and *$p < 0.05$, **$p < 0.01$ and ***$p < 0.0001$ as compared with drug dispersion.

HepG2 cells (23% and 32% respectively) (Fig. 6(a)) at the low exposure time employed, and this inhibitory effect resulted in the targeting of these cancer cells, since the viability of HUVECs was not affected with the same treatment (Fig. 6(b)). Altogether, these results indicate that the specific attachment, uptake, and effective action of the loaded drug, using both functionalized NPs, is restricted to cancer cells, enabling

the prevention of side effects in healthy vascular cells. This is also well illustrated by the result that any variation in the concentration employed of the free drug alone, for Phx or STB (Figs. 7(a) and 7(c), respectively), did not alter the viability of HepG2 cells, at the tested concentrations.

In contrast, biotinylated NPs with Phx did show a linear dose-response curve for viability of HepG2 cells, until a maximum threshold of activity at a concentration of 20.81 µM (Fig. 7(b)). Therefore, we concluded that 20.81 µM of Phx was the more adequate concentration of drug to load in our targeted NPs, in order to achieve a good balance between specificity, efficacy, and biosafety. On the other hand, biotinylated NPs with STB also exhibited a proportional profile of cell viability inhibition in HepG2 cells, until the maximum effective dose of STB of 18.77 µM (Fig. 7(d)). Since increasing the loading of NPs with a dose of STB higher than 18.77 µM was technically unviable, and the use of higher concentrations than this would be closer to other reported studies with free drug [42], these data suggest that the best concentration of STB for loading to NPs would be between 9.38-18.77 µM. The use of biotinylated NPs in this range of STB concentration would represent the best choice to preserve high activity and selectivity, without causing possible toxic effects in healthy vascular endothelial cells. Therefore, both treatments with biotinylated NPs demonstrated suitability of these nanocarriers to successfully target and deliver different multi-target anticancer drugs for human hepatocellular carcinoma, with an excellent endovascular biosafety profile. On the whole, this selective treatment appears to be useful to overcome the limitations of current therapy for human hepatocellular carcinoma due to harmful side effects. Moreover, the simultaneous incorporation of drug and plasmid may also help physicians to refine surgical procedures, delimitating affected areas of liver by means of imaging techniques. Recently, there has been a trend towards the improvement of diagnostic technologies through the detection of specific fluorescent dyes. Our dual carriers can also reach this goal, behaving as platforms targeted to cancer, for DNA delivery with a powerful inducible mammalian expression system to stain cancer cells with GFP.
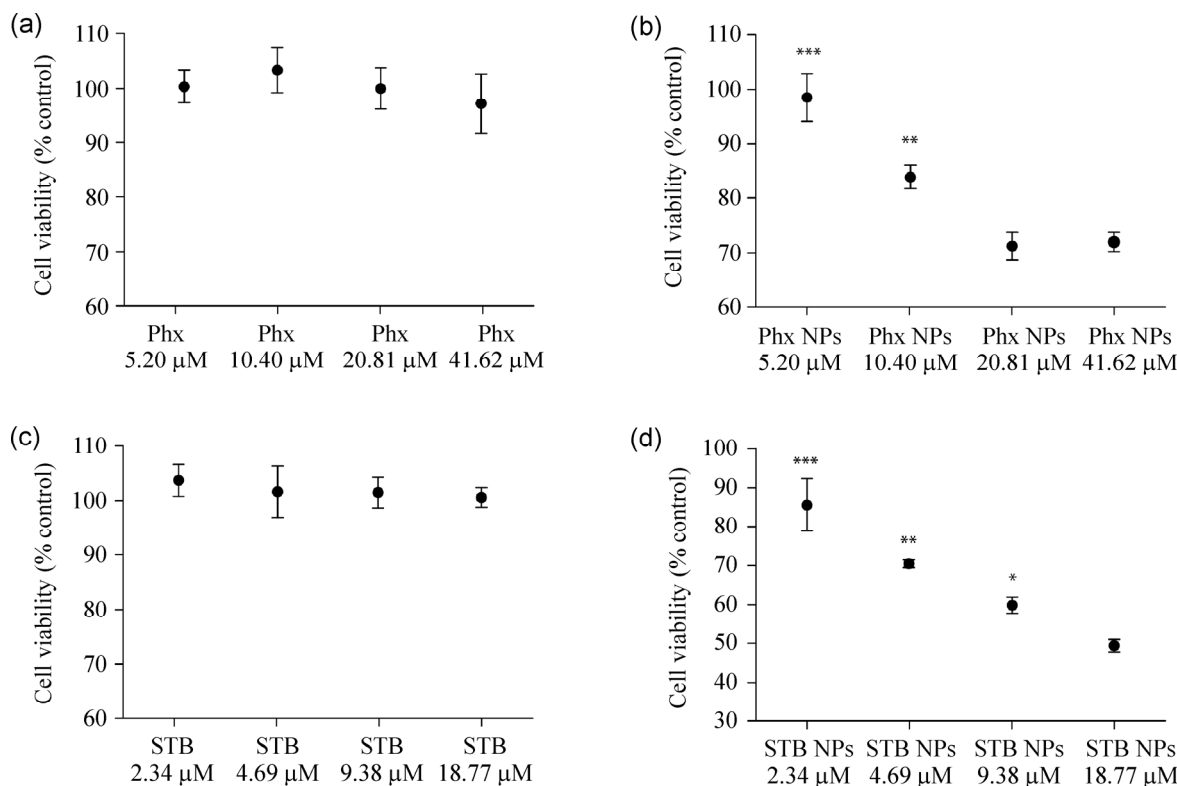
Figure 7 Dose response-curves of antitumor drug dispersions and anticancer drug-loaded polyurethane-urea (PUR) nanoparticles (NPs) in human hepatocellular carcinoma cells (HepG2). (a) phenoxodiol (Phx) dispersions and (b) Phx loaded-biotinylated PUR NPs, at drug concentrations of 41.62, 20.81, 10.40, and 5.20 μM (2 mg·mL^{-1}, 1 mg·mL^{-1}, 500 μg·mL^{-1} and 250 μg·mL^{-1} of NPs). (c) sunitinib malate (STB) solution and (d) STB loaded-biotinylated PUR NPs, at drug concentrations of 18.77, 9.38, 4.69, and 2.34 μM (2 mg·mL^{-1}, 1 mg·mL^{-1}, 500 μg·mL^{-1} and 250 μg·mL^{-1} of NPs). Each filled circle represents the mean ± SEM. $*p < 0.05$, $**p < 0.01$ and $***p < 0.0001$ as compared with anticancer drug or anticancer drug-loaded NPs at 41.62 μM or 18.77 μM for Phx and STB, respectively.

4   Conclusions

In summary, we have designed biotinylated PUR NPs from O/W nano-emulsions in water/biotin/ P80/MCT/ IPDI systems, which selectively target human hepatoma cells and are able to deliver plasmid DNA and drugs for therapy and diagnosis in hepatocellular carcinoma. This dual theranostic tool takes advantage of the very high requirements of cancer cells for biotin, in order to grow exponentially. We have demonstrated, through the immunocytofluorescence studies performed here, that these NPs are incorporated and accumulated in the perinuclear and nuclear area of human hepatoma cells. Accordingly, the use of biotinylated NPs/plasmid reporter complexes allowed easy fluorescent detection of hepatoma cells, but not human vascular endothelial cells. For this reason, the privileged subcellular localization of these NPs in cancer cells makes these nanocarriers good candidates for targeted gene therapy in cancer. Moreover, we have demonstrated that the additional combination of these biotinylated NPs with multi-target drugs, such as phenoxodiol or sunitinib, reduced the cell viability of hepatoma cells but not human endothelial cells, thereby exhibiting high specificity for tumor cells. Altogether our results support the concept that these NPs represent a combination of good theranostic properties as well as a good biosafety profile. Therefore, these nanocarriers will be useful in enhancing the efficiency of current therapy of human hepatocellular carcinoma and other cancers, minimizing side effects and furthermore, allowing simultaneous cancer delineation for precise tumor resection.

Acknowledgements

Electronic Supplementary Material: Supplementary material including additional Figures and Tables corresponding to physicochemical and biological characterization of biotinylated polyurethane described in the section "Design and characterization of biotinylated polyurethane-urea nanoparticles loaded with a reporter gene-containing plasmid and either sunitinib or phenoxodiol" is available in the online version of this article at http://dx.doi.org/10.1007/s12274-014-0678-6.

References

[1] Brannon-Peppas, L.; Blanchette, J.O. Nanoparticle and targeted systems for cancer therapy. *Adv. Drug. Deliver. Rev.* **2004**, *56*, 1649–1659.

[2] Wang, S. Y.; Kim, G.; Lee, Y.-E.; Hah, H. J.; Ethirajan, M.; Pandey, R. K.; Kopelman, R. Multifunctional biodegradable polyacrylamide nanocarriers for cancer theranostics—A "see and treat" strategy. *ACS Nano* **2012**, *6*, 6843–6851.

[3] Morral-Ruíz, G.; Melgar-Lesmes, P.; Solans, C.; García-Celma, M. J. Multifunctional polyurethane-urea nanoparticles to target and arrest inflamed vascular environment: Apotential tool for cancer therapy and diagnosis. *J. Control. Release* **2013**, *171*, 163–171.

[4] Morral-Ruíz, G.; Solans, C.; García, M. L.; García-Celma, M. J. Formation of pegylated polyurethane and lysine-coated polyurea nanoparticles obtained from O/W nano-emulsions. *Langmuir* **2012**, *28*, 6256–6264.

[5] Moghimi, S. M.; Hunter, A. C.; Murray, J. C. Long-circulating and target-specific nanoparticles: Theory to practice. *Pharmacol. Rev.* **2001**, *53*, 283–318.

[6] Bonzani, J. C.; Adhikari, R.; Houshyar, S.; Mayadunne, R.; Gunatillake, P.; Stevens, M. M. Synthesis of two-component injectable polyurethanes for bone tissue engineering. *Biomaterials* **2007**, *28*, 423–433.

[7] Brannon-Peppas, L.; Blanchette, J. O. Nanoparticle and targeted systems for cancer therapy. *Adv. Drug. Deliver. Rev.* **2012**, *64*, 206–212.

[8] Blanpain, C. Tracing the cellular origin of cancer. *Nat. Cell.* *Biol.* **2013**, *15*, 126–134.

[9] Vadlapudi, A. D.; Vadlapatla, R. -K.; Pal, D.; Mitra, A. K. Biotin uptake by T47D breast cancer cells: Functional and molecular evidence of sodium-dependent multivitamin transporter (SMVT). *Int. J. Pharm.* **2013**, *441*, 535–543.

[10] Soininen, S. K.; Lehtolainen-Dalkilic, P.; Karppinen, T.; Puustinen, T.; Dragneva, G.; Kaikkonen, M. U.; Jauhiainen, M.; Allart, B.; Selwood, D. L.; Wirth, T. et al. Targeted delivery via avidin fusion protein: Intracellular fate of biotinylated doxorubicin derivative and cellular uptake kinetics and biodistribution of biotinylated liposomes. *Eur. J. Pharm. Sci.* **2012**, *47*, 848–856.

[11] Zempleni, J. Uptake, localization, and noncarboxylase roles of biotin. *Annu. Rev. Nutr.* **2005**, *25*, 175–196.

[12] Fang, J.; Nakamura, H.; Maeda, H. The EPR effect: Unique features of tumor blood vessels for drug delivery, factors involved, and limitations and augmentation of the effect. *Adv. Drug Deliv. Rev.* **2011**, *63*, 136–151.

[13] Sangiovanni, A.; Del Ninno, E.; Fasani, P.; De Fazio, C.; Ronchi, G.; Romeo, R.; Morabito, A.; De Franchis, R.; Colombo, M. Increased survival of cirrhotic patients with a hepatocellular carcinoma detected during surveillance. *Gastroenterology* **2004**, *126*, 1005–1014.

[14] Llovet, J. M.; Di Bisceglie, A. M.; Bruix, J.; Kramer, B. S.; Lencioni, R.; Zhu, A.X.; Sherman, M.; Schwartz, M.; Lotze, M.; Talwalkar, J. et al. Design and endpoints of clinical trials in hepatocellular carcinoma. *J. Natl. Cancer Inst.* **2008**, *100*, 698–711.

[15] Newell, P.; Toffanin, S.; Villanueva, A.; Chiang, D. Y.; Minguez, B.; Cabellos, L.; Savic, R.; Hoshida, Y.; Lim, K. H.; Melgar-Lesmes, P. et al. Ras pathway activation in hepatocellular carcinoma and anti-tumoral effect of combined sorafenib and rapamycin in vivo. *J. Hepatol.* **2009**, *59*, 725–733.

[16] Forner, A.; Llovet, J. M.; Bruix, J. Hepatocellular carcinoma. *Lancet* **2012**, *379*, 1245–1255.

[17] Lu, C. H.; Willner, B.; Willner, I. DNA nanotechnology: From sensing and DNA machines to drug-delivery systems. *ACS Nano* **2013**, *7*, 8320–8332.

[18] Singh, M.; Ariatti, M. Targeted gene delivery into HepG2 cells using complexes containing DNA, cationized asialoorosomucoid and activated cationic liposomes. *J. Control. Release* **2003**, *92*, 383–394.

[19] Morral-Ruíz, G.; Melgar-Lesmes, P.; García, M. L.; Solans, C.; García-Celma, M. J. Design of biocompatible surface-modified polyurethane and polyurea nanoparticles. *Polymer* **2012**, *53*, 6072–6080.

[20] Chen, C.; Heng, Y. C.; Yu, C. H.; Chan, S. W.; Cheung, M. K.; Yu, P. H. F. In vitro cytotoxicity, hemolysis assay, and biodegradation behaviour of biodegradable

poly(3-hydroxybutyrate)–poly(ethylene glycol)–poly (3-hydroxybutyrate) nanoparticles as potential drug carriers. *J. Biomed. Mater. Res. A* **2008**, *87*, 290–298.

[21] Faivre, S.; Zappa, M.; Vilgrain, V.; Boucher, E.; Douillard, J.-Y.; Lim, H. Y.; Kim, J. S.; Im, S. A.; Kang, Y.-K.; Bouattour, M. et al. Changes in tumor density in patients with advanced hepatocellular carcinoma treated with sunitinib. *Clin. Cancer Res.* **2011**, *17*, 4504–4512.

[22] Silasi, D.-A.; Alvero, A. B.; Rutherford, T. J.; Brown, D.; Mor, G. Phenoxodiol: Pharmacology and clinical experience in cancer monotherapy and in combination with chemotherapeutic drugs. *Expert Opin. Pharmacother.* **2009**, *10*, 1059–1067.

[23] Perrault, S. D.; Walkey, C.; Jennings, T.; Fischer, H. C.; Chan, W. C. W. Mediating tumour targeting efficiency of nanoparticles through design. *Nano Lett.* **2009**, *9*, 1909–1915.

[24] Yuan, F.; Dellian, M.; Fukumura, D.; Leunig, M.; Berk, D. A.; Torchilin, V. P.; Jain, R. K. Vascular permeability in a human tumor xenograft: Molecular size dependence and cutoff size. *Cancer Res.* **1995**, *17*, 3752–3756.

[25] Hobbs, S. K.; Monsky, W. L.; Yuan, F.; Roberts, W. G.; Griffith, L.; Torchilin, V. P.; Jain, R. K. Regulation of transport pathways in tumor vessels: Role of tumor type and microenvironment. *Proc. Natl. Acad. Sci. U. S. A.* **1998**, *95*, 4607–4612.

[26] Melgar-Lesmes, P.; Morral-Ruíz, G.; Solans, C.; García-Celma, M. J. Quantifying the bioadhesive properties of surface-modified polyurethane-urea nanoparticles in the vascular network. *Colloids Surf. B* **2014**, *118*, 280–288.

[27] Vonarbourg, A.; Passirani, C.; Saulnier, P.; Benoit, J. P. Parameters influencing the stealthiness of colloidal drug delivery Systems. *Biomaterials* **2006**, *27*, 4356–4373.

[28] Rapiti, E.; Verkooijen, H. M.; Vlastos, G.; Fioretta, G.; Neyroud-Caspar, I.; Sappino, A. P.; Chappuis, P. O.; Bouchardy, C. Complete excision of primary breast tumor improves survival of patients with metastatic breast cancer at diagnosis. *J. Clin. Oncol.* **2006**, *24*, 2743–2749.

[29] Orringer, D. A.; Koo, Y.-E. L.; Chen, T.; Kim, G.; Hah, H. J.; Xu, H.; Wang, S. Y.; Keep, R.; Philbert, M. A.; Kopelman, R. et al. In vitro characterization of a targeted, dye-loaded nanodevice for intraoperative tumor delineation. *Neurosurgery* **2009**, *64*, 965–972.

[30] Ferrari, M. Cancer nanotechnology: Opportunities and challenges. *Nat. Rev. Cancer* **2005**, *5*, 161–171.

[31] Eyüpoglu, I. Y.; Hore, N.; Savaskan, N. E.; Grummich, P.; Roessler, K.; Buchfelder, M.; Ganslandt, O. Improving the extent of malignant glioma resection by dual intraoperative visualization approach. *PLoS ONE* **2012**, *7*, e44885.

[32] Pedraza, C. E.; Basset, D. C.; McKee, M. D.; Nelea, V.; Gbureck, U.; Barralet, J. E. The importance of particle size and DNA condensation salt for calcium phosphate nanoparticle transfection. *Biomaterials* **2008**, *29*, 3384–3392.

[33] Kaneda, Y. Virosome: A novel vector to enable multi-modal strategies for cancer therapy. *Adv. Drug Deliv. Rev.* **2012**, *64*, 730–738.

[34] Glendenning, J. L.; Barbachano, Y.; Norman, A. R.; Dearnaley, D. P.; Horwich, A.; Huddart, R. A. Long-term neurologic and peripheral vascular toxicity after chemotherapy treatment of testicular cancer. *Cancer* **2010**, *116*, 2322–2331.

[35] Gan, H. K.; Seruga, B.; Knox, J. J. Sunitinib in solid tumors. *Expert Opin. Investig. Drugs.* **2009**, *18*, 821–834.

[36] Killock, D. Kidney cancer: Sunitinib has similar efficacy irrespective of age in mRCC. *Nat. Rev. Clin. Oncol.* **2014**, *11*, 122.

[37] Lopergolo, A.; Nicolini, V.; Favini, E.; Dal Bo, L.; Tortoreto, M.; Cominetti, D.; Folini, M.; Perego, P.; Castiglioni, V.; Scanziani, E. et al. Synergistic cooperation between sunitinib and Cisplatin promotes apoptotic cell death in human medullary thyroid cancer. *J. Clin. Endocrinol. Metab.* **2014**, *99*, 498–509.

[38] Herst, P. M.; Petersen, T.; Jerram, P.; Baty, J.; Berridge M. V. The antiproliferative effects of phenoxodiol are associated with inhibition of plasma membrane electron transport in tumour cell lines and primary immune cells. *Biochem. Pharmacol.* **2007**, *74*, 1587–1595.

[39] Aguero, M. F.; Facchinetti, M. M.; Sheleg, Z.; Senderowicz, A. M. Phenoxodiol, a novel isoflavone, induces G1 arrest by specific loss in cyclin-dependent kinase 2 activity by p53-independent induction of p21$^{WAF1/CIP1}$. *Cancer Res.* **2005**, *65*, 3364–3373.

[40] Kamsteeg, M.; Rutherford, T.; Sapi, E.; Hanczaruk, B.; Shahabi, S.; Flick, M. Phenoxodiol—an isoflavone analog—induces apoptosis in chemoresistant ovarian cancer cells. *Oncogene* **2003**, *22*, 2611–2620.

[41] Yao, C.; Wu, S. J.; Li, D. M.; Wang, Z. Y.; Yang, Y. J.; Yang, S. C.; Gu, Z. P. Co-administration phenoxodiol with doxorubicin synergistically inhibit the activity of sphingosine kinase-1 (SphK1), a potential oncogene of osteosarcoma, to suppress osteosarcoma cell growth both *in vivo* and *in Vitro*. *Molecular Oncology* **2012**, *6*, 392–404.

[42] Mendel, D. B., Laird, A. D.; Xin, X. H.; Louie, S. G.; Christensen, J. G.; Li, G. M.; Schreck, R. E.; Abrams, T. J.; Ngai, T. J.; Lee, L. B. et al. In vivo antitumor activity of SU11248, a novel tyrosine kinase inhibitor targeting vascular endothelial growth factor and platelet-derived growth factor receptors: Determination of a pharmacokinetic/ pharmacodynamic relationship. *Clin. Cancer Res.*, **2003**, *9*, 327–337.